

Article

Sensing Pre- and Post-Ecdysis of Tropical Rock Lobsters, *Panulirus ornatus*, Using a Low-Cost Novel Spectral Camera

Charles Sutherland ^{1,*}, Alan D. Henderson ¹, Dean R. Giosio ¹, Andrew J. Trotter ² and Greg G. Smith ²

¹ School of Engineering, University of Tasmania, Sandy Bay, TAS 7005, Australia; alan.henderson@utas.edu.au (A.D.H.); dean.giosio@utas.edu.au (D.R.G.)

² Institute for Marine & Antarctic Studies (IMAS), University of Tasmania, Taroona, TAS 7053, Australia; andrew.trotter@utas.edu.au (A.J.T.); gregory.smith@utas.edu.au (G.G.S.)

* Correspondence: charles.sutherland@utas.edu.au

Abstract: Tropical rock lobsters (*Panulirus ornatus*) are a highly cannibalistic species with intermoult animals predominantly attacking animals during ecdysis (moulting). Rapid, positive characterisation of pre-ecdysis lobsters may open a pathway to disrupt cannibalism. Ecdysial suture line development is considered for pre-ecdysis recognition with suture line definition compared for intermoult and pre-ecdysis lobsters emerged and immersed, using white, near ultraviolet (365 nm), near infrared (850 nm), and specialty SFH 4737 broadband IR LEDs against a reference of intermoult lobsters with no suture line development. Difficulties in acquiring suture line images prompted research into pre-ecdysis characterisation from the lobster's dorsal carapace, due to its accessibility through a culture vessel's surface. In this study, a novel low-cost spectral camera was developed by coordinating an IMX219 image sensor, an AS7265x spectral sensor, and four SFH 4737 broadband infrared LEDs through a single-board computer. Images and spectral data from the lobster's dorsal carapace were acquired from intermoult, pre-ecdysis, and post-ecdysis lobsters. For the first time, suture line definition was found to be enhanced under 850 nm, 365 nm, and SFH 4737 LEDs for immersed lobsters, while the 850 nm LED achieved the best suture line definition of emerged lobsters. Although the spectral camera was unable to characterise pre-ecdysis, its development was validated when a least squares regression for binary classification decision boundary successfully separated 86.7% of post-ecdysis lobsters. Achieving post-ecdysis characterisation is the first time the dorsal carapace surface has been used to characterise a moult stage for palinurid lobsters.



Citation: Sutherland, C.; Henderson, A.D.; Giosio, D.R.; Trotter, A.J.; Smith, G.G. Sensing Pre- and Post-Ecdysis of Tropical Rock Lobsters, *Panulirus ornatus*, Using a Low-Cost Novel Spectral Camera. *J. Mar. Sci. Eng.* **2024**, *12*, 987. <https://doi.org/10.3390/jmse12060987>

Academic Editor: Sergei Chernyi

Received: 13 April 2024

Revised: 25 May 2024

Accepted: 10 June 2024

Published: 12 June 2024



Copyright: © 2024 by the authors. Licensee MDPI, Basel, Switzerland. This article is an open access article distributed under the terms and conditions of the Creative Commons Attribution (CC BY) license (<https://creativecommons.org/licenses/by/4.0/>).

1. Introduction

Tropical rock lobsters (*Panulirus ornatus*) have significant aquaculture potential; however, as a juvenile animal, they are highly cannibalistic, which provides a challenge for the large-scale propagation of this species. Cannibalism events predominantly occur for *P. ornatus* during the process of ecdysis (moulting), where the moulting animals are cannibalised by intermoult animals [1]. An element missing from current strategies is the ability to automatically identify pre-ecdysis juvenile lobsters, which is currently limited to manual inspection. Technology designed to sense pre-ecdysis may provide an opportunity to disrupt cannibalism and is thus the primary focus of this study. Achieving rapid sorting, or possibly an automated solution capable of in situ sensing of pre-ecdysis lobsters, is a desirable long-term outcome because excessive manual handling stresses lobsters, interferes with feed intake, and increases the risk of limb autotomy, which can retard the growth rate of the lobsters [2,3].

A comprehensive review of the literature found few precedent works on the subject of pre-ecdysis sensing of lobsters. Garland and Sekretta [4] found that the join between the head and thorax of a nephropid lobster, *Homarus americanus*, would darken under

infrared light with increasing levels of blood protein, but no such marker has been reported for palinurid (spiny) lobsters. Sutherland et al. [5] use photographic methods to appraise markers of pre-ecdysis by comparing intermoult and pre-ecdysis lobsters using visual appraisal and digital image analysis in the HSV color space. Sutherland et al. [5] found that suture line development was a pre-ecdysis marker, but its formation was disguised by surrounding pigment when captured in images using only visible light. Sutherland et al. [6] used an exploratory approach testing five non-destructive ultrasound transducers and found a signal segment strongly associated with intermoult lobsters formed a basis to distinguish intermoult and pre-ecdysis lobsters. This study intends to expand on the foundation of pre-ecdysis sensing possibilities and inform and guide further research into pre-ecdysis sensing, rather than a thorough investigation of a single sensing opportunity.

Moult stage classifications as defined by Sutherland et al. [6] are used for this study. Pre-ecdysis juvenile lobsters are defined as those on the day of ecdysis, with fully developed suture lines, while the intermoult stage is defined as one-week post-ecdysis extending to the earliest external signs of approaching ecdysis. Sutherland et al. [5] report that early signs of approaching ecdysis are noted by ventral surface pigment absorption and darkening of the region between the thorax and abdomen, and the darkening of the pleopods and uropods. Comparative analysis is used to find distinct differences between data collected from the intermoult and pre-ecdysis groups that could form the basis of a pre-ecdysis sensor [6].

Affordability is a key requirement for industry due to foreseen replicated installation throughout a culture facility [6]. Illuminating the lobster's surface with narrowband light sources is a simple, low-cost way to explore the interaction of varying light conditions and the low-cost IMX219 NOIR (Sony Semiconductor Manufacturing Corporation, Kumamoto, Japan) image sensor chosen for use in this study [7,8].

Suture lines must develop for each moult as they are key to survival by enabling escape from the old exoskeleton [9,10]. Suture lines on small lobsters are difficult to discern visually, making pre-ecdysis identification imprecise and onerous, and requiring experience for manual identification. An image of a clear, conspicuous suture line could improve both speed and accuracy of manual identification to facilitate the separation of animals, thus reducing the load on production staff and increasing productivity [11]. Improving suture definition would also increase the likelihood of success of an *in situ* computer vision pre-ecdysis detector by making a clear distinction between intermoult and pre-ecdysis lobsters. Lowe [12] explains that feature extraction is simplified for images with less clutter, which highlights the advantages of processing images of well-defined features on predominantly smooth backgrounds.

Comparing the definition of the suture line against its visible light appearance will establish if any advantage of distinction is gained by using light outside the visible light spectrum. Further comparisons with lobsters prior to suture line development can enrich the understanding of how varying the light conditions affect the definition with which suture lines appear on images of juvenile lobsters. Complications for suture line detection *in situ* are gaining a side-perspective view of lobsters from cameras on the bottom or sides of culture vessels, and the positioning of the legs which obscures the region of suture line formation.

The noted complications associated with suture detection prompted consideration of other methods for pre-ecdysis sensing. Disconnecting the exoskeleton in preparation for moulting is a known marker of pre-ecdysis which may result in a biochemical change on the dorsal carapace surface, and near-infrared spectroscopy is a tool able to detect such changes [13]. Changes observed on the cephalothorax of *H. americanus* under infrared light support an exploratory investigation of the dorsal carapace using infrared techniques for *P. ornatus* [4]. Pre-ecdysis detection from the dorsal carapace surface of palinurid lobsters is desirable as it is accessible via entry through the culture vessel's surface [6].

A hyperspectral snapshot camera in combination with an infrared light source may be suited for infrared spectrographic sensing of the dorsal carapace surface. Infrared light above 1400 nm penetrates only millimetres through water, meaning that much of the capabil-

ity of such a camera is wasted. A further key consideration is its cost of around USD 15,000. An exploratory low-cost novel spectral camera was built at a cost of USD 610 [14]. Simultaneous data collection from an IMX219 NOIR image sensor and an AS7265x spectral sensor (ams OSRAM AG, Premstätten, Austria) was coordinated with a single board computer (SBC). Using broadband infrared illumination from SFH 4737 LEDs (ams OSRAM AG, Regensburg, Germany) and placing the camera lens in the centre of the AS7265x sensors creates an exploratory, novel low-cost spectroscopy sensor to attempt pre-ecdysis detection from the dorsal carapace [14]. Aquino et al. [15] demonstrated that the combination of SFH 4737 LEDs with an AS7265x spectral sensor was able to create a low-cost tool to evaluate the fat content of olives, while Noguera et al. [16] assessed the ripeness of grapes and achieved promising results.

Post-ecdysis lobsters, defined in this study as being lobsters on the day after ecdysis, are an extra group included for comparison in testing the novel spectral camera. The post-ecdysis dorsal carapace surface is distinguished from intermoult and pre-ecdysis by being unmineralized [17,18]. Successful recognition of the post-ecdysis dorsal carapace would provide encouragement that the novel spectral camera may have broader applications in other research endeavours, and opportunistically provide a documented post-ecdysis detector.

This study aims to appraise the comparative definition of suture lines in images against baseline images of intermoult lobsters under varying lighting conditions using a IMX219 NOIR image sensor. This study then aims to investigate and report on the performance and characteristics of SFH 4737 LEDs and the AS7265x spectral sensor when operated as components in a novel spectral camera based around the IMX219 NOIR image sensor. We also aim to assess the reliability of operation, and data consistency of the novel spectral camera while being tested as a sensor of pre-ecdysis, and/or post-ecdysis from the dorsal carapace surface of *P. ornatus*.

2. Materials and Methods

2.1. Test Animals

2.1.1. Animal Husbandry

The study was undertaken at the Institute for Marine and Antarctic Studies (IMAS), University of Tasmania, Taroona, over a duration of four months. Twelve hatchery-bred and -reared juvenile *P. ornatus* were utilised in this study. Lobsters had a carapace length and weight range of 35.9–50.4 mm and 46.9–123.1 g, respectively. The lobsters were of mixed sex, with 5 females and 7 males in the population. The lobsters were maintained in a communal culture vessel ($2.52\text{ m} \times 0.96\text{ m} \times 0.38\text{ m}$ —length \times width \times height; volume 920 L), on recirculating seawater, temperature $26 \pm 0.5^\circ\text{C}$, salinity 34.0 ± 0.8 , pH 8.2 ± 0.1 , and with culture vessels receiving 3 water exchanges h^{-1} . Lobsters were fed twice daily with proprietary formulated pellet at a rate of 3.5% dry weight of animal body weight, adjusted to satiation. Cleaning of the tanks and removal of uneaten feed was performed via siphon prior to each feeding event.

2.1.2. Moult Stages for Comparison

The moult stage groups for comparison are as follows: (1) Intermoult lobsters, in this instance defined as one-week post-ecdysis extending to the earliest external signs of pre-ecdysis; (2) Pre-ecdysis, lobsters on the day of ecdysis with fully developed suture lines; (3) Post-ecdysis, lobsters on the day after ecdysis. Sutherland et al. [5] provides further details on the timing of externally visible indications of approaching ecdysis and moult stage classification.

2.2. System Components and Construction

2.2.1. Host Single-Board Computer

The host SBC was a Jetson Nano development kit (Rev 2B) (NVIDIA Corporation, Santa Clara, CA, USA) running Jetpack 5.6. Nvgstcapture-1.0 (NVIDIA Corporation,

Santa Clara, CA, USA) is a Jetson image capture and camera control application supplied with the Jetpack SDK. Nvgstcapture-1.0 natively produces a live preview stream to a display and can simultaneously capture images. The system was built on to Nvgstcapture-1.0 to include control of the light sources via the system's GPIO. UART communication with the AS7265x spectral sensor (ams OSRAM AG, Premstätten, Austria) was added using the Termios libraries using programmed AT commands through a USB UART interface. Imaging via a CSI/MIPI interface and spectral data collection via USB allowed near-simultaneous (<100 ms) operation.

2.2.2. Camera

The IMX219 NOIR (Sony Semiconductor Manufacturing Corporation, Kumamoto, Japan) image sensor was used for all image collection. The sensor was mounted on an Arducam carrier board and connected to the host system via a CSI/MIPI interface. Arducam (Arducam Technology Co., Ltd., Suzhou, China) supply the IMX219 NOIR sensor with a motorised focus lens that is adjustable from the host system via the I²C connection included in the CSI/MIPI interface specification [19]. The camera was left in its default configuration with automatic exposure mode, permitting time to adjust to test light conditions before image acquisition. Although available with a NOIR designation from Arducam and Raspberry Pi (Raspberry Pi Foundation, Cambridge, UK), the sensitivity information of this camera is incomplete. Sony's datasheet does not specify the full NOIR sensitivity of the sensor's RGB channels beyond 700 nm, with Sony indicating that this sensor is not a designated IR sensor ([20], Internal comms). Pagnutti et al. [7] independently reviewed the specifications of this sensor on a Raspberry Pi V2 fixed-focus module, but also did not report the sensitivity beyond 700 nm. A wider channel sensitivity bandwidth is reported for other Sony sensors. The IMX335 (Sony Semiconductor Manufacturing Corporation, Kumamoto, Japan) image sensor has a similar sensitivity pattern to the IMX219 NOIR, between 400 and 700 nm, with the expanded sensitivity plot showing how the three channels have overlapping sensitivity in the near infrared, just beyond 800 nm [21]. It was expected that the channel sensitivity of the IMX219 NOIR would behave similarly, albeit with reduced sensitivity levels, due to the similarity of the underlying semiconductor and RGB filter properties.

2.2.3. Light Sources for Suture Line Imaging

Four illuminating light sources for suture line imaging were LED SJ-3W-CW cool white LEDs (visible light) (Shenzhen Ipixel LED Light Co., Ltd., Shenzhen, China), LZ4-00R408 850 nm LEDs (NIR) (LED Engin, Inc., San Jose, CA, USA), LZ1-00UV0R 365 nm LEDs (NUV) (LED Engin, Inc., San Jose, CA, USA), and SFH 4737 LEDs (IR broadband) (ams OSRAM AG, Regensburg, Germany).

2.2.4. Near-Infrared Spectroscopy Light Source

SFH 4737 LEDs were used as the spectroscopy light source. The SFH 4737 LEDs operated for 3 s bursts to meet the requirements for integration of the AS7265x sensors. LED 2000 driver demonstration boards (Model STEVAL-ILL051V1, STMicroelectronics N.V., Geneva, Switzerland) were left in their default configuration for driving the SFH 4737 LEDs at 700 mA to generate a high intensity light. The operational parameters of the LEDs varied from those given in the datasheet (350 mA, 10 mS pulse) [22]. The relative emission spectrum of the LEDs under operational conditions was recorded with a SpectralEvolution RS-8800 spectrometer (Spectral Evolution Inc., Haverhill, MA, USA) off a 127 × 127 mm (5 × 5 inch) white 99% Spectralon reflectance panel (Labsphere Inc., North Sutton, NH, USA). The measured curve of the LED relative radiant intensity emission spectrum was overlaid on the characteristic relative emission spectrum from the datasheet for comparison. The SFH 4737 LEDs were mounted on purpose built aluminium PCBs for heat control.

2.2.5. Spectral Sensor

An AS7265x 18-channel spectral array was used to capture spectral data. The AS7265x sensors were set to their maximum integration time of 708.9 ms. The AS7265x gain control is a linear multiplier and was set to its maximum value of 64. Test samples were taken to ensure the 16-bit channel data registers did not saturate and cause data loss. Each aperture of the three AS7265x sensors was covered with Tsujiden D121UP diffraction film (Tsujiden Co., Ltd., Tokyo, Japan) to ensure adequate light diffusion from the target at close range.

The AS7265x datasheet shows that each channel has an associated integration function that covers a bandwidth of light wavelengths [23]. Each of the 18 integration functions is presented relative to its own peak value, resulting in a common scale between 0 and 1. This presentation overlooks the effects of relative channel sensitivity. A full calibration to a known light source is impractical with integration functions that are neither defined nor scaled to relative sensitivity. However, relative channel sensitivity can be investigated by testing with a calibrated light source.

Channel sensitivity was assessed with the low-cost spectral camera fitted in its housing. A Labsphere Helios (Model USLR-D12L-NANS, Labsphere Inc., North Sutton, NH, USA) integration sphere with a 150 W lamp at 50% power was used as the test source. Raw data from test shots taken by the AS7265x were corrected using the formula:

$$g(\lambda) = \frac{L(\lambda)}{\frac{R_{DN}^{(\lambda)\text{total}} - R_{DN}^{(\lambda)\text{dark}}}{IT}} \quad (1)$$

where $g(\lambda)$ is calibration gain, L is calibrated source radiance, R_{DN} is measured total signal or dark current of the test sensor, and IT is the integration time of the test sensor. All test data were analysed as relative values because the continuous wavelength readout from the Helios integration sphere could not be mapped to the channel outputs of the AS7265x due to the undefined channel integration functions.

Four reference values were required to relatively adjust, align, and compare the known curve of the test light source, the readings of the test light source from the AS7265x, the gain correction curve, and the gain-corrected readings of the test light source from the AS7265x. The four reference points were as follows: (1) The test light source data were made relative to the value at 940 nm as this was the highest value in the relevant wavelength domain. (2) Readings of the test light source from the AS7265x were made relative to the 810 nm channel value as this was the highest recorded value. (3) Gain correction curve values were made relative to the 810 nm value as this value was close to the median value of the gain correction curve and it also aligned with the AS7265x data reference in point 2. (4) The gain-corrected AS7265x readings of the test light source was made relative to the 940 nm channel value as this was the highest value and aligned the AS7265x corrected readings to the known test light source curve. The derived gain correction curve can be used to assess the extent to which channel sensitivity contributes to the acquired data.

2.2.6. Low-Cost Spectral Camera

The low-cost spectral camera was constructed by mounting the camera lens through a hole central to the placement of the three AS7265x sensors on the AMS AS7265x demonstration board. Four SFH 4737 LEDs surrounded the low-cost spectral camera in a purpose-built black HDPE housing with acrylic windows. Each LED was surrounded by a parabolic reflector and fitted into a separate tube. The four tubes were mounted in the housing to focus the individual light beams to a point 75 mm directly in front of the camera lens and AS7265x spectral sensors (Figure 1). A manual action button was used to trigger the following capture sequence: (1) ambient LEDs off; (2) SFH 4737 LEDs on; (3) integration delay/camera exposure adjustment; (4) near-simultaneous image and spectral capture; (5) SFH 4737 LEDs off; (6) ambient LEDs on.



Figure 1. The HDPE waterproof housing (95×142 mm) with glued in clear acrylic windows. The four light tubes are arranged to focus the four light sources 75 mm beneath the sensors. (A) A SFH 4737 LED surrounded by a parabolic reflector; (B) the three AS7265x chips covered with Tsujiden D121UP diffraction film with the camera lens visible through the centre hole.

2.3. Suture Line Imaging

Imaging the suture lines facilitated image comparisons under the four light sources outlined in Section 2.2.3. Suture line images from pre-ecdysis lobsters and baseline images from intermoult lobsters were collected for comparison. Each light source was assessed for definition of the suture line when compared with the baseline image. Comparative image sets were acquired from emerged and immersed lobsters.

2.3.1. Emerged Suture Line Imaging

Emerged suture line images were taken to assess suture line appearance in the circumstance of camera-assisted manual sorting. In this circumstance, only the assessment of RGB images was deemed suitable, given the simplicity of using a direct camera feed. To obtain clear images of emerged lobsters, the lobsters were secured to an elevated platform, and images were acquired from the side. The elevated platform allowed the legs to fall away from the region of suture development so its full extent could be captured in images.

2.3.2. Immersed Suture Line Imaging

Immersed suture line imaging was considered as a circumstance aligned with in situ automated detection of the suture line. Lobsters were placed in water filled 3 mm clear acrylic tubes, so the sides of the lobsters were accessible for imaging. The suture line's appearance was compared on the complete RGB image, and on each color channel presented in greyscale.

2.4. Low-Cost Spectroscopy Camera

Intermoult, pre-ecdysis, and post-ecdysis lobsters were sampled for comparative spectral and image data. The use of GPIO controlled ambient (white) lighting allowed the camera's on-screen preview to be used to align the low-cost spectral camera with distinct

spines and edges on the dorsal surface of the lobster. Image and spectral data were captured from the dorsal surface of lobsters held on a platform and submerged in a blackened tank of seawater after switching to illumination from SFH 4737 LEDs. Multiple readings were taken to ensure suitably comparable readings and images were acquired from each lobster.

2.4.1. Spectral Sampling NIR Reflectance Analysis

Only the seven longest wavelength channels, which include all the NIR channels, of the AS7265x were used for analysis. The visible light channels, particularly in blue, are affected by the colored pigments of the lobster's surface, which varies naturally in a population and are not considered for analysis. The AS7265x NIR channel raw data were plotted by lobster for each of the three sample groups to assess the variability of the data between lobsters and groups. The spectral distribution from the dorsal carapace was assessed for apparent changes that occurred within the distributions of the three sample groups, while the seven long wavelength channel values were summed to assess the relative reflectance of all NIR light. Means for each group and the gain-corrected means for each group were all plotted on the same axis to assess the effect of channel sensitivity on the mean distribution shape.

2.4.2. Spectral Sampling Image Analysis

All images were compared as the complete color image and split into grayscale representations of each RGB channel to better understand the effect of the SFH 4737 emission spectrum has on image presentation at the IMX219 sensor.

Green channel image analysis of the dorsal carapace proceeded by creating a dorsal carapace ROI through setting all pixels outside the dorsal carapace boundary to black. A threshold value of 35 (out of 255) was chosen as the threshold to distinguish dark and illuminated pixels in the ROI. The green channel images were normalised to percentage of illuminated pixels using the count of illuminated pixels and the total count of ROI pixels.

2.4.3. Spectral Sampling Statistical Analysis

Achieving either pre-ecdysis or post-ecdysis characterisation using the spectral camera requires establishing that either the pre-ecdysis or post-ecdysis groupings can be statistically separable from the other groups. Statistical methods have been applied to check the separation of the three lobster groups using the NIR reflectance data, the green channel pixel percentage data, and using both data streams in combination. The statistical analysis was performed using the R programming language. One-way ANOVAs were performed for the reflectance of the summed AS7265x NIR raw channel data (Section 2.4.1), and green channel pixel percentage illumination (Section 2.4.2) across the three sample groups. All data were checked for conformance to the normal distribution with a Shapiro–Wilk test, and for homogeneity with Bartlett's test. The ANOVAs were grouped by stage, and significant results were assessed with a Tukey HSD post hoc comparison. Significance was accepted at level $p < 0.05$.

To check for correlation between the NIR reflectance data and the green channel illuminated pixel percentage data, a Pearson's correlation coefficient was performed. A correlation analysis of the combined intermoult and pre-ecdysis data was performed, with the post-ecdysis data correlated separately.

The green channel percentage of pixel illumination data was plotted against the NIR reflectance data with the stage groups as individual series. Least squares regression for binary classification was used to establish a decision boundary to separate post-ecdysis and the combined intermoult and pre-ecdysis stage groups on the plot. The model used was:

$$\delta(X) = \begin{cases} 1 X^T \beta + \beta_0 \geq 0 \\ -1 X^T \beta + \beta_0 < 0 \end{cases} \quad (2)$$

where X is a vector of the two independent variables of green channel pixel percentage illumination and infrared reflectance, β is a vector of slope coefficients from the least squares regression, and β_0 is the intercept coefficient.

3. Results

3.1. Emerged Suture Line Imaging

With the lobster emerged, the suture line is detectable on pre-ecdysis images under all four lighting conditions. Under the NIR and the SFH 4737 LEDs, the suture line is well defined along its entire length as the detail and contrast of other surface structures of the lobster are suppressed. Visible and NUV lighting maintains the definition of non-suture line textures and contrast on the surface of the lobster (representative images are shown in Figure 2). The suture remains distinct from baseline intermoult images because the suture path between the carapace and the branchiostegite is white during intermoult and becomes dark when the suture lines form. However, the posterior section of suture development on the carapace has a similar appearance to intermoult due to similarity with a band of brown pigment normally present on the intermoult branchiostegite.

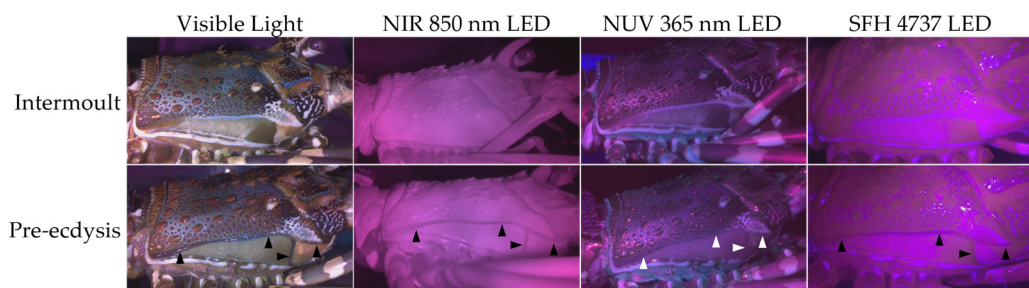


Figure 2. The appearance of suture lines of staged *Panulirus ornatus* under four light sources with image capture on a Sony IMX219 NOIR image sensor. Arrows on the pre-ecdysis images indicate the suture line.

3.2. Immersed Suture Line Imaging

With the lobster immersed and imaged using visible light, the presence of brown pigmentation on the posterior branchiostegite increases the uncertainty of suture line identification because the formed suture line is only defined by having a darker appearance when compared to the pigmentation in intermoult images. NIR, NUV, and SFH 4737 LEDs show the suture line is clear and distinct from the intermoult images, with obvious darkening occurring in the suture line's posterior section. These light sources do not reflect the brown pigmentation of the posterior branchiostegite, which improves the definition of the suture line when it is present in this region. Suture line obstruction by the legs is evident in all images, with the anterior section of the suture being most affected, supporting the preferred focus on the posterior carapace (Figure 3).

The RGB channel breakdown from the IMX219 NOIR image sensor shows little difference between the images of the three channels for visible light images. Under visible light, the posterior suture line appears slightly darker than the equivalent appearance of pigmentation present in the baseline images. Under NIR light, the suppression of surface contrast and features enhances the definition and contrast of the suture line on all color channels compared to baseline images. The green channel image is noticeably grainier than the red and blue channel images when viewed at high resolution but appears unchanged at the resolution of Figure 3. The NUV light source creates a dark suture line which contrasts with a clear white line of intact integument of the intermoult images. The blue channel is marginally brightest overall, but both the red and blue channels capture contrast and detail of the lobster's surface features, albeit with reduced definition in the red channel image. NUV lighting does not convey information in the green channel with the images being too dark for any definition in the image.

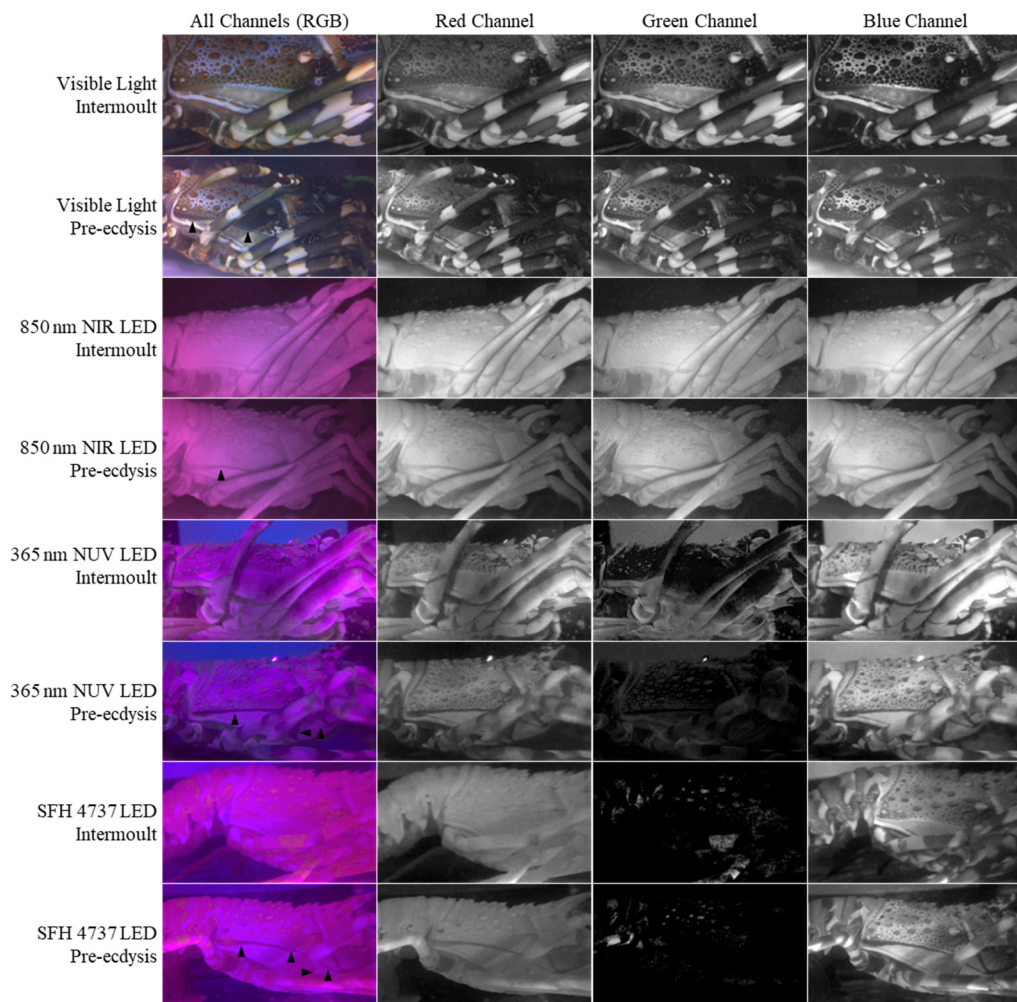


Figure 3. The appearance of the posterior suture line region of submerged *Panulirus ornatus* illuminated by four different light sources with image capture on a Sony IMX219 NOIR image sensor. Representative RGB images are broken into greyscale representations of the red, green, and blue color channels. Arrows on the pre-ecdysis RGB images indicate the suture line.

The SFH 4737 LEDs produce images on the IMX219 NOIR image sensor with a red channel that closely resembles the NIR image, and a blue channel that closely resembles the NUV image blue channel. The red channel strongly suppresses contrast and detail leaving a mostly smooth image, while the blue channel captures the full contrast and detail of the carapace surface. The green channel conveys no information about the suture line as it is too dark, although regions of pixels corresponding with spines and pigmentation bands on the legs are activated and appear “grainy”.

3.3. Spectral Analysis

3.3.1. SFH 4737 Relative Emission Spectrum

The system relative emission spectrum is a close match to the emission published in the SFH 4737 product datasheet (Figure 4). The infrared performance beyond 850 nm appears slightly degraded in the configuration used for sampling. A maximum deviation of approximately 3% occurs at 950 nm. The maximum deviation between 500 and 700 nm is approximately 0.035%.

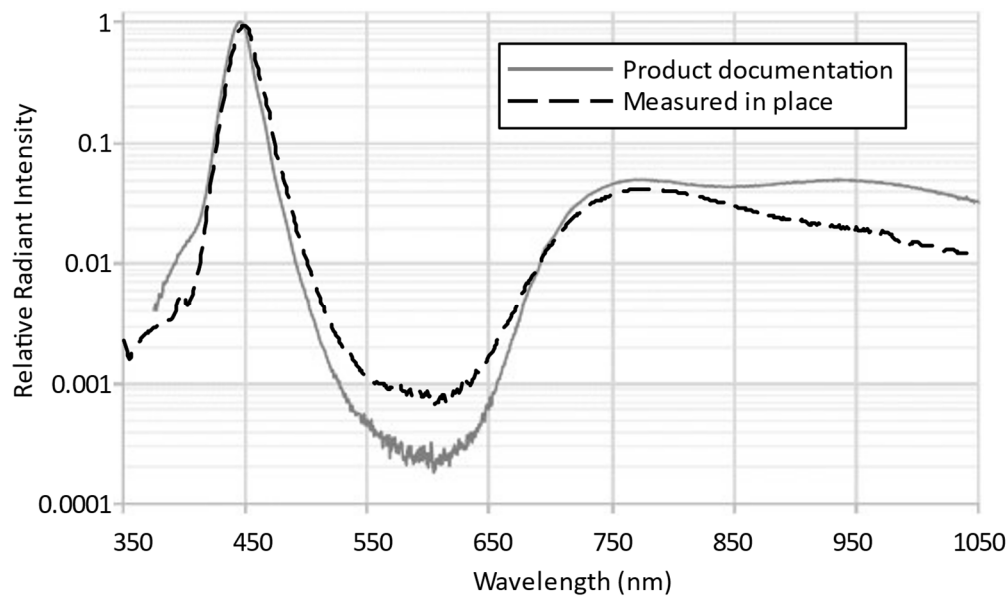


Figure 4. The relative emission spectrum of the system SFH-4737 LEDs vs. the product's stated relative emission spectrum [22]. Logarithmic Y-axis, with a maximum variation of 3% at 950 nm.

3.3.2. AS7265x Calibration

A gain correction curve to map the AS7265x channel output to a calibration light source was generated. The deviation of the gain correction curve from its reference of 1 is indicative of the relative spectral sensitivities of the channels on the AS7265x. Values greater than 1 indicate reduced relative channel sensitivity, while values less than 1 indicate heightened relative channel sensitivity. The calibration curve has increased channel sensitivity in the 410, 435, and 460 nm blue light channels. Channel sensitivity to infrared at the 900 and 940 nm channels is reduced, with the 940 nm channel being less than half as sensitive as the median level (Figure 5).

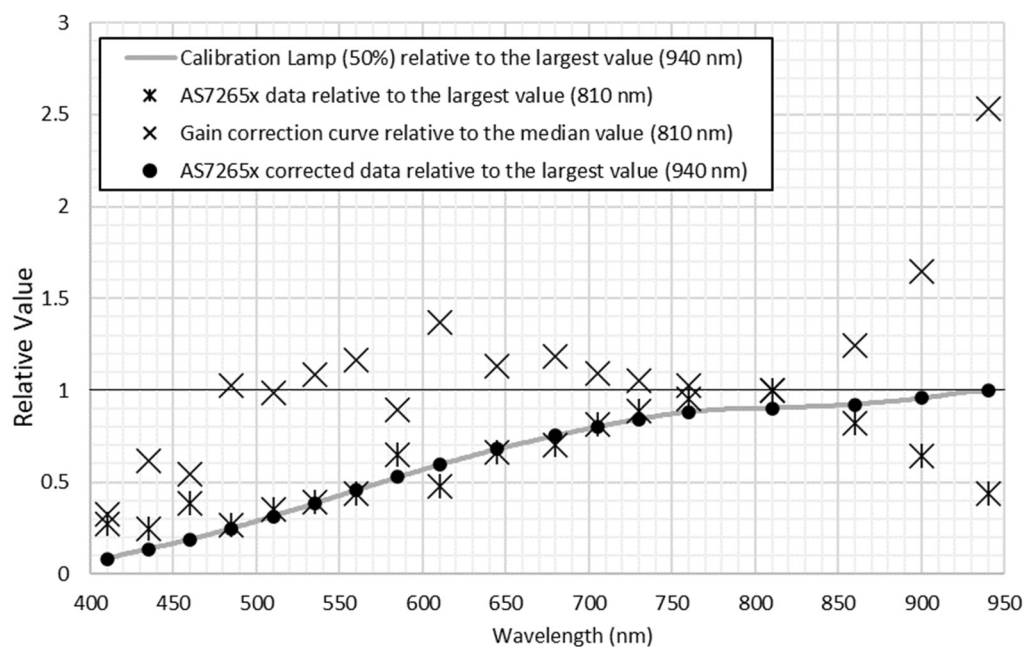


Figure 5. Fitting the AS7265x channel sensitivities to a known calibrated light source (Helios integration sphere) using relative values.

3.3.3. Dorsal Surface Imaging Using the Low-Cost Camera

The appearance of the dorsal carapace in red and blue channel images shows no obvious differences between the intermoult, pre-ecdysis, and post-ecdysis groups. Reiterating the results from suture line imaging using the SFH 4737 lights, the red channel images have strongly suppressed contrast and appear as a NIR image, while the blue channel images have high contrast and feature definition and appear as a NUV blue channel image. The green channel on images of the dorsal carapace produces a third view, where the green channel from suture line images was mostly dark (Figure 6). The intermoult and pre-ecdysis green channel images have similar pixel illumination for each lobster, but the post-ecdysis green channel image of each lobster has reduced pixel illumination levels (Figure 7).

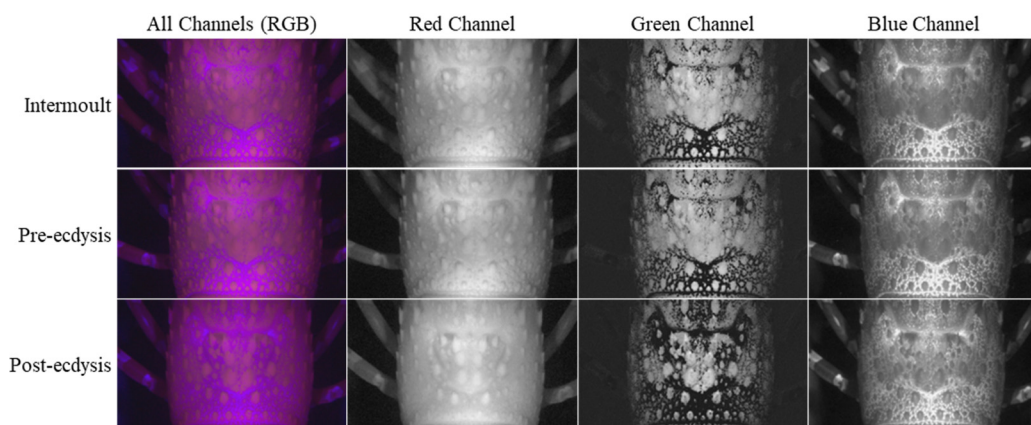


Figure 6. Close-up view of the posterior dorsal surface of a *Panulirus ornatus* lobster using four SFH 4737 LEDs for illumination with image capture on a Sony IMX219 NOIR image sensor. The RGB images are broken into greyscale representations of its red, green, and blue color channels. Each row is a separate moult cycle stage.

Overall, the one-way ANOVA result of a green channel illuminated pixel percentage value analysis was significant. The group results were as follows: intermoult $56.3\% \pm 17.7\%$; pre-ecdysis $53.9\% \pm 16.3\%$; post-ecdysis $27.3\% \pm 13.1\%$. ($F = 12.47$; d.f. = 2.33; and $p < 0.0001$). The Tukey HSD post hoc comparison showed significance between the post-ecdysis values and both the intermoult and pre-ecdysis values ($p = 0.0002$ and $p = 0.0006$ respectively). However, the intermoult and pre-ecdysis values were not significantly different ($p = 0.9254$). The intermoult and pre-ecdysis pixel illumination values were combined for further comparisons with the post-ecdysis values.

3.3.4. Dorsal Surface Spectral Analysis Using the Low-Cost Camera

The spectral distribution around the NIR channels of the AS7265x formed a characteristic peak at the 810 nm channel when illuminated by SFH 4737 LEDs. The level of reflectivity increases steadily from the 705 nm channel with an increasing wavelength to the 810 nm channel and then declines to the 940 nm channel. No change in the absorption characteristic of the dorsal carapace is evident because all channel values remained in a proportionally similar position to each other. The highest variation in reflectivity occurs at the central 810 nm channel, with both margins (705 and 940 channels) showing only small variability. The variability of the channels in the midpoints between the centre and each edge was proportional to their distance from the centre (Figure 8).

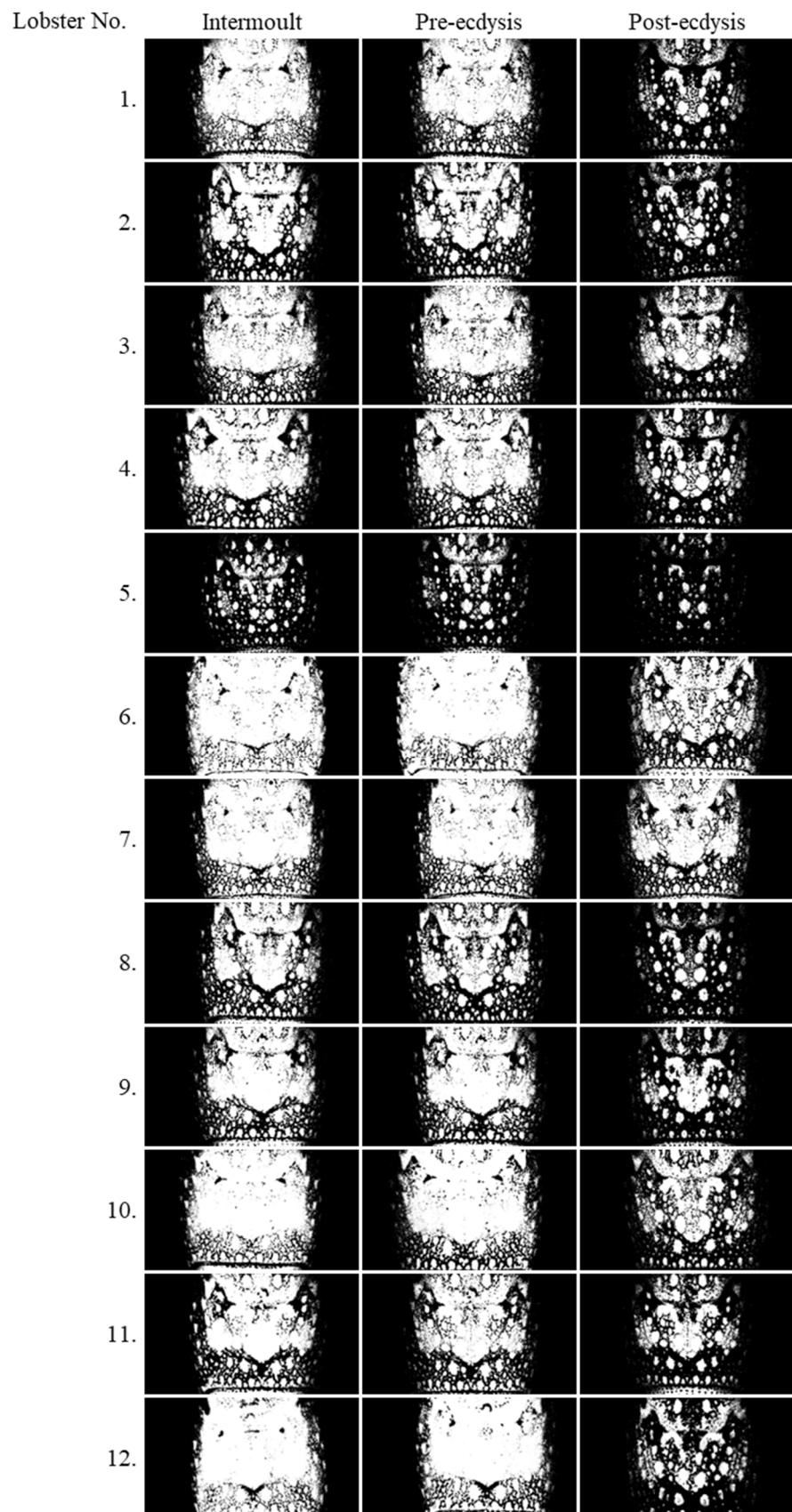


Figure 7. Representative green channel images of the dorsal carapace of the twelve sample *Panulirus ornatus* lobsters using SFH 4737 LEDs. The images have been masked outside the dorsal carapace, and a threshold of 35 (out of 255) has been applied.

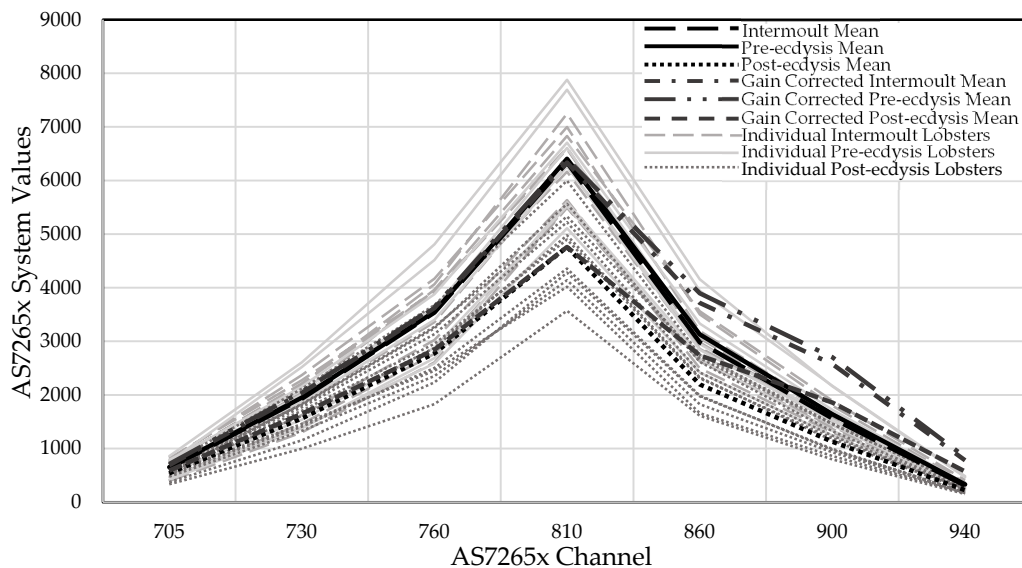


Figure 8. AS7265x NIR channel raw system value spectral distribution plots from the dorsal carapace surface of *Panulirus ornatus* lobsters during growth, pre-ecdysis, and post-ecdysis stages. High variability is evident from the individual spectral distributions.

The individual lobster traces show consistency of proportional placement of each spectral channel on the AS7265x (Figure 8). An overall change in NIR reflectivity is apparent due to the proportional scaling of all points. On average, lobsters are less reflective to NIR light at post-ecdysis. The one-way ANOVA of infrared light reflectance from the surface of lobsters showed a significant result ($F = 9.35$; d.f. = 2.27; and $p = 0.0008$). Group results were as follows (summed AS7265x NIR channel raw data): intermoult $17,287 \pm 2184$; pre-ecdysis $17,659 \pm 3270$; post-ecdysis $13,185 \pm 2379$. The Tukey HSD post hoc comparison showed significance between the post-ecdysis values and both the intermoult and pre-ecdysis values ($p = 0.0036$ and $p = 0.0021$ respectively). However, the NIR reflectance of intermoult and pre-ecdysis lobsters was not significantly different ($p = 0.9487$). The intermoult and pre-ecdysis NIR reflectivity values were combined for further comparisons with the post-ecdysis group.

Applying the gain correction leaves the distinct peak reflection at 810 nm intact and has little effect on the overall shape of the spectral curve, particularly on the lower peak sensitivity channels. Channel sensitivity has its largest influence on the 860 nm and 900 nm peak channel. The effect of gain calibration appears reduced at the 940 nm peak channel due to the relatively low values recorded. Channel sensitivity itself does not create the reflectivity peak at the 810 nm peak channel.

3.3.5. Correlation of Illuminated Pixel Percentage and NIR Abundance

Correlation between illuminated pixel percentage and NIR abundance was not seen for the combined intermoult and pre-ecdysis values ($r = -0.0034$ and $p = 0.9890$), nor the post-ecdysis values ($r = 0.0782$ and $p = 0.8191$).

3.3.6. Scatterplot of Illuminated Pixel Percentage and NIR Abundance

The scatterplot of illuminated pixel percentage values against NIR abundance values shows intermingling of the intermoult and pre-ecdysis values. The post-ecdysis values generally gather away from the intermoult and pre-ecdysis values. The least squares regression model ($R^2 = 0.5804$; RSE = 0.6581 with d.f. 27) produced a binary classification decision boundary line with formula:

$$y = -0.0059x + 126.25 \quad (3)$$

This boundary correctly classifies 26 of 30 (86.7%) of the sample lobsters (Figure 9).

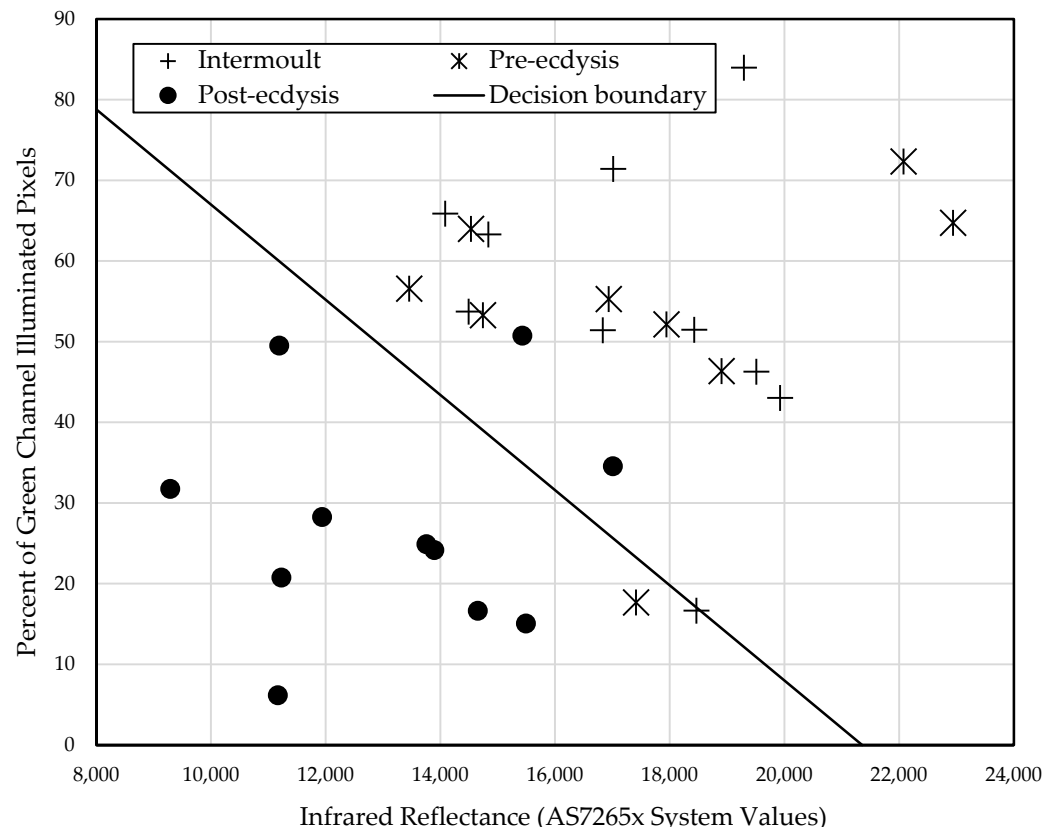


Figure 9. Scatterplot of percentage of green channel illuminated pixels and infrared reflectance by stage from the dorsal carapace of *Panulirus ornatus*. A linear regression for binary classification decision boundary was determined to separate the post-ecdysis values from the combined growth and pre-ecdysis values.

4. Discussion

Extensive stock losses due to conspecific cannibalistic interactions in culture vessels is driving a need to detect the signs of pre-ecdysis quickly and accurately, whether the lobster is in, or out, of the culture vessel. Suture line development and nutrient and mineral reabsorption are key pre-ecdysis events that may enable pre-ecdysis characterisation with a sensor. Suture line development occurs visibly, allowing assessment via manual inspection, or via a computer vision algorithm. While nutrient and mineral re-absorption does not alter the visual appearance of the dorsal carapace, it may alter the surface chemical composition and thus light absorption properties on the lobster's surface. Altered light absorption properties would create an opportunity to use spectroscopy to characterise pre-ecdysis. A low-cost spectral sensing solution is required for practical reasons. The availability of low-cost components, SBCs, and rapid development coupled with comparative analysis enable the creation and assessment of novel solutions.

Real advantages in suture line imaging were gained by testing a variety of light sources with the Sony IMX219 NOIR camera. Clarifying the presence of the suture simplifies detecting approaching ecdysis and is a step towards the ultimate goal of identifying pre-ecdysis *in situ*. Overall, the use of visible light is the least preferred method to create a well-defined image of the suture line. NIR light's ability to flatten contrast and detail creates a smooth background against which the suture line becomes well defined. NUV light produces a well-defined suture line for immersed lobsters while maintaining the details of the lobster's surface.

The ability of the SFH 4737 LEDs to produce three different views simultaneously on the three camera channels creates benefits for the use of this light source, particularly in conjunction with computer vision. Using the red and blue channel images could allow parallel inference from two models for improved detection accuracy. Parallel inference with re-combination is used for combining RGB image data with depth information for improved inference accuracy [24].

The low-cost camera was effective at aligning the target via the on-screen preview allowing comparable datasets to be acquired. The data generated by the low-cost camera also had high repeatability and consistency, which is supported by Ducanchez et al. [25], who report good repeatability when using the AS7265x sensors, and Pagnutti et al. [7] report that the Raspberry Pi camera module V2 has stable operational characteristics. The spectral readings consistently created a proportionally scaled output which has low variability in the proportional placement of the datapoints. The spectral distribution shape, particularly the reflectivity peak on the 810 nm channel, was unexplained either by variations in the emission spectrum from the SFH 4737 LEDs under our operational conditions, or by the channel sensitivity biases introduced by the AS7265x spectral sensor. In the absence of an alternative explanation, it appears that *P. ornatus* strongly reflects NIR light around 810 nm.

Using an SBC was beneficial in this study as it allowed the green channel of the camera and the NIR channels of the AS7265x to be captured simultaneously and combined to a single two-dimensional dataset. Dorsal surface characterisation of post-ecdysis lobsters was demonstrated using the two-dimensional dataset with the creation of a least squares regression decision boundary to correctly classify 86.7% of lobsters on the two-dimensional plane created by the AS7265x NIR reflectivity data and the camera's green channel pixel illumination percentage data. Higher classification rates are unlikely due to high variability amongst the sample lobster population, particularly of the dorsal surface excretion responsible for green channel pixel illumination. Sutherland et al. [5] noted a high variability of ventral surface color due to phenotypic and exogenic effects, which is likely applicable here.

A second benefit from the use of an SBC is control of invisible light sources. Cummins et al. [26] show that *Panulirus argus* have light sensitivity from 360 nm to approximately 600 nm, which may trigger photo avoidance behaviours. This observation coupled with the spectral reflectivity observation that NIR reaches a reflectivity peak near 810 nm from the surface of lobsters indicate that an invisible NIR light source may be most suitable for monitoring lobsters in culture vessels with a camera. We demonstrated effective on/off light control from the same Jetson Nano used for data collection using only simple additional circuits and readily available components.

The third benefit of SBCs is flexible configuration. The Jetson Nano development kit carrier board is equipped with a GPIO that has 2 PWM GPIO pins, UART (serial), I²C, and SPI communications, and dual CSI/MIPI camera connectors. Dimming control of the lights was unused in this study, but easily implemented by swapping the GPIO output to PWM and using the dimming control input of the STEVAL-ILL051V1 LED driver boards (STMicroelectronics N.V., Geneva, Switzerland). This allows for full automation of light control with the development of object detection models. The manual action button could be substituted by an inference trigger to momentarily change the Jetson Nano's light and camera configuration to capture the best possible images for pre-ecdysis characterisation and reduce high intensity infrared light exposure while monitoring.

Upgrading both the spectral and image sensors are options to increase spectral resolution, addressing the observation that pre-ecdysis changes on the surface of the dorsal carapace were insufficient to detect using the low-cost spectral sensing system as developed. The AS7421 (ams OSRAM AG, Premstätten, Austria) has 64 NIR channels between 700 and 1000 nm [27], while image sensor technology is advancing steadily from the different vendors, including a wider variety of specialty sensors.

The Jetson Nano has dual display outputs on the development kit carrier board allowing this system to form the basis of a manual identification workstation based on suture line detection. Clarification of the suture can be used for manual sorting by production

workers in the interim as development continues towards in situ detection. Clear vision of the suture lines facilitates fast and accurate sorting and reduces handling and time spent out of water which are important factors in manual sorting. Using a live stream to a computer monitor and replacing the shutter release button with a foot pedal, an operator would have two hands free to gently hold and position the lobster in front of a camera and light source, placed behind a protective screen. A system that makes manual sorting viable in a production setting could have an immediate impact in reducing losses to conspecific cannibalism.

5. Conclusions

In this study of 12 juvenile *P. ornatus*, images were taken and grouped into three moult stages measured relative to the observed day of ecdysis: intermoult, pre-ecdysis, and post-ecdysis lobsters. For the first time, it was shown that formed suture lines can be captured in images with greater definition by using light sources outside visible light with lobsters emerged and immersed.

The IMX219 NOIR image sensor and narrowband 850 nm LED combined to flatten contrast and reduce detail, as well as suppress surface pigmentation in images. The suture line was made conspicuous by appearing against a mostly featureless background. The clarified suture line may simplify manual sorting and is also a step towards in situ automated pre-ecdysis characterisation.

The novel low-cost spectral camera developed specifically in this study showed promising operational characteristics collecting many comparable images and spectral samples with a high level of consistent, reproduced data. Separate interactions of reduced green channel pixel percentage illumination and reduced NIR reflectance from the dorsal surface combined to enable the characterisation of post-ecdysis from the dorsal surface of *P. ornatus* for the first time. This finding providing encouragement that the exploratory creation and testing of this novel spectral camera may have application in other research endeavours.

This study has shown that combining image, spectral data, and specialty light sources into a single two-dimension data stream, it is easily possible to re-configure and tune the system from the variety of available components. Combining different low-cost sensors on the same base platform provided a low-cost analogue of typically expensive equipment.

This innovative design of a low-cost spectral camera showed that the dorsal surface of *P. ornatus* remains stable between intermoult and pre-ecdysis despite nutrient and mineral absorption occurring within the integument. In the absence of a contradictory finding, the dorsal surface stability of twelve *P. ornatus* juveniles into pre-ecdysis excludes the spectrographic determination of pre-ecdysis, regardless of the equipment used.

Author Contributions: Conceptualization, C.S.; methodology, C.S.; software, C.S.; formal analysis, C.S.; investigation, C.S.; resources, C.S., A.D.H. and G.G.S.; data curation, C.S.; writing—original draft preparation, C.S.; writing—review and editing, C.S., A.D.H., D.R.G., A.J.T. and G.G.S.; supervision, A.D.H., D.R.G., A.J.T. and G.G.S.; project administration, C.S., A.D.H. and G.G.S.; funding acquisition, G.G.S. All authors have read and agreed to the published version of the manuscript.

Funding: This research was conducted by the Australian Research Council Industrial Transformation Hub for Sustainable Onshore Lobster Aquaculture (project number IH190100014). The views expressed herein are those of the authors and are not necessarily those of the Australian Government or the Australian Research Council.

Institutional Review Board Statement: Ethical review and approval were waived for this study due to research on invertebrates is currently exempt from ethics approval as per the current Australian code for the care and use of animals for scientific purposes. “The Code applies to the care and use of all live non-human vertebrates and cephalopods”. Decapod crustaceans do not fall within these categories.

Informed Consent Statement: Not applicable.

Data Availability Statement: Data are available on request.

Acknowledgments: We would like to express appreciation for the technical assistance at IMAS, including Mathew Allan, Charlotte Levi, Jose Garcia Lafuente, Nigel Coombes, and Ross Goldsmid, and technical assistance at the School of Engineering from Andrew Bylett, Rodrigo Ximeno, Ellie Jane, Simon Hogwood, Jon Rodden, and Rick Barrett. We are grateful to Yukiko Burns from the Australia Japan Society, and Hachimure from TSUJIDEN Co., Ltd. for organising and supplying the D121UP diffusion film used in this study.

Conflicts of Interest: The authors declare no conflicts of interest. The funders had no role in the design of the study; in the collection, analyses, or interpretation of data; in the writing of the manuscript; or in the decision to publish the results.

References

1. Kelly, T.R.; Giosio, D.R.; Trotter, A.J.; Smith, G.G.; Fitzgibbon, Q.P. Cannibalism in Cultured Juvenile Lobster *Panulirus Ornatus* and Contributing Biological Factors. *Aquaculture* **2023**, *576*, 739883. [[CrossRef](#)]
2. Emery, T.J.; Hartmann, K.; Green, B.S.; Gardner, C. Handled with Care: Minimal Impacts of Appendage Damage on the Growth and Productivity of the Southern Rock Lobster (*Jasus Edwardsii*). *Fish. Res.* **2016**, *175*, 75–86. [[CrossRef](#)]
3. Frisch, A.J.; Hobbs, J.-P.A. Effects of Autotomy on Long-Term Survival and Growth of Painted Spiny Lobster (*Panulirus Versicolor*) on the Great Barrier Reef, Australia. *Mar. Biol.* **2011**, *158*, 1645–1652. [[CrossRef](#)]
4. Garland, J.J.; Sekretta, G. Imaging for Determination of Crustacean Physical Attributes. U.S. Patent US20150359205A1, 17 December 2015.
5. Sutherland, C.; Henderson, A.; Trotter, A.J.; Giosio, D.; Smith, G. Assessing Sensing Techniques for Detecting Markers of Approaching Ecdysis in Juvenile Tropical Rock Lobsters, *Panulirus ornatus*. *Aquac. Eng.* **2023**, *102*, 102342. [[CrossRef](#)]
6. Sutherland, C.; Henderson, A.; Holloway, D.; Trotter, A.J.; Giosio, D.; Smith, G. A Survey of NDT Ultrasound Transducers for Sensing Pre-Moult Tropical Rock Lobsters, *Panulirus ornatus*. *Appl. Acoust.* **2024**, *223*, 110073. [[CrossRef](#)]
7. Pagnutti, M.; Ryan, R.E.; Cazenavette, G.; Gold, M.; Harlan, R.; Leggett, E.; Pagnutti, J. Laying the Foundation to Use Raspberry Pi 3 V2 Camera Module Imagery for Scientific and Engineering Purposes. *J. Electron. Imaging* **2017**, *26*, 013014. [[CrossRef](#)]
8. Malchow, D. Imaging in the Shortwave Infrared (SWIR) for Industrial Applications: When Visible Imaging Comes up Short, SWIR Can Be the Answer. *Adv. Imaging* **2007**, *22*, 30–36.
9. Aiken, D.E. Molting and Growth. In *The Biology and Management of Lobsters*; Academic Press: New York, NY, USA, 1980; Volume 1, pp. 91–163, ISBN 0-12-177401-5.
10. Passano, L.M. Molting and Its Control. In *The Physiology of Crustacea*; Waterman, T.H., Ed.; Academic Press: New York, NY, USA, 1960; Volume 1, pp. 473–536, ISBN 978-0-12-395628-6.
11. Jones, C.M. Tropical Spiny Lobster Aquaculture Development in Vietnam, Indonesia and Australia. *J. Mar. Biol. Assoc. India* **2010**, *52*, 304–315.
12. Lowe, D.G. Distinctive Image Features from Scale-Invariant Keypoints. *Int. J. Comput. Vis.* **2004**, *60*, 91–110. [[CrossRef](#)]
13. Beć, K.B.; Grabska, J.; Huck, C.W. Near-Infrared Spectroscopy in Bio-Applications. *Molecules* **2020**, *25*, 2948. [[CrossRef](#)] [[PubMed](#)]
14. Sutherland, C.R.; Henderson, A.; Giosio, D.; Trotter, A.; Smith, G. Synchronising an Imx219 Image Sensor and As7265x Spectral Sensor to Make a Novel Low-Cost Spectral Camera. *Preprints* **2024**, *2024040897*. [[CrossRef](#)]
15. Aquino, A.; Noguera, M.; Millan, B.; Mejías, A.; Ponce, J.M.; Andújar, J.M. A Preliminary Evaluation of a Low-Cost Multispectral Sensor for Non-Destructive Evaluation of Olive Fruits' Fat Content. In *XLIII Jornadas de Automática: Libro de Actas: 7, 8 y 9 de Septiembre de 2022, Logroño (La Rioja)*; Servizo de Publicacións da UDC: A Coruña, Spain, 2022; pp. 475–478, ISBN 978-84-9749-841-8.
16. Noguera, M.; Millan, B.; Andújar, J.M. New, Low-Cost, Hand-Held Multispectral Device for In-Field Fruit-Ripening Assessment. *Agriculture* **2022**, *13*, 4. [[CrossRef](#)]
17. Roer, R.; Dillaman, R. The Structure and Calcification of the Crustacean Cuticle. *Am. Zool.* **1984**, *24*, 893–909. [[CrossRef](#)]
18. Travis, D.F.; Friberg, U. The Deposition of Skeletal Structures in the Crustacea: VI. Microradiographic Studies of the Exoskeleton of the Crayfish *Orconectes virilis* Hagen. *J. Ultrastruct. Res.* **1963**, *9*, 285–301. [[CrossRef](#)] [[PubMed](#)]
19. Arducam NoIR IMX219-AF Programmable/Auto Focus IR Sensitive Camera Module for Nvidia Jetson Nano. Arducam. 2023. Available online: <https://www.arducam.com/product/b0189-arducam-noir-imx219-af-programmable-auto-focus-ir-sensitive-camera-module-nvidia-jetson-nano/> (accessed on 9 June 2024).
20. Arducam IMX219 Datasheet. 2016. Available online: <https://docs.arducam.com/Raspberry-Pi-Camera/Native-camera/source/IMX219DS.PDF> (accessed on 20 May 2024).
21. FRAMOS FSM-IMX335 Datasheet. Available online: <https://www.framos.com/wp-content/uploads/FSM-IMX335-Datasheet.pdf> (accessed on 10 August 2023).
22. ams-OSRAM AG SFH 4737 Datasheet. Available online: <https://look.ams-osram.com/m/576f284cd3c20cb4/original/SFH-4737.pdf> (accessed on 9 June 2023).
23. ams-OSRAM AG AS7265x Smart 18-Channel VIS to NIR Spectral_ID 3-Sensor Chipset with Electronic Shutter. Available online: <https://look.ams-osram.com/m/76ce4c0d80cd1565/original/AS7265x-DS000612.pdf> (accessed on 9 June 2023).
24. He, L.; Wang, G.; Hu, Z. Learning Depth from Single Images with Deep Neural Network Embedding Focal Length. *IEEE Trans. Image Process.* **2018**, *27*, 4676–4689. [[CrossRef](#)] [[PubMed](#)]

25. Ducanchez, A.; Moinard, S.; Brunel, G.; Bendoula, R.; Héran, D.; Tisseyre, B. The AS7265x Chipset as an Alternative Low-Cost Multispectral Sensor for Agriculture Applications Based on NDVI. In *Proceedings of the Sense the Real Change: Proceedings of the 20th International Conference on Near Infrared Spectroscopy*; Chu, X., Guo, L., Huang, Y., Yuan, H., Eds.; Springer Nature: Singapore, 2022; pp. 201–206.
26. Cummins, D.R.; Chen, D.-M.; Goldsmith, T.H. Spectral Sensitivity of the Spiny Lobster, *Panulirus argus*. *Biol. Bull.* **1984**, *166*, 269–276. [CrossRef]
27. ams-OSRAM AG AS7421 64-Channel Hyperspectral NIR Sensor. Available online: <https://look.ams-osram.com/m/1164a4e1da5c19a9/original/AS7421-DS000667.pdf> (accessed on 9 June 2023).

Disclaimer/Publisher’s Note: The statements, opinions and data contained in all publications are solely those of the individual author(s) and contributor(s) and not of MDPI and/or the editor(s). MDPI and/or the editor(s) disclaim responsibility for any injury to people or property resulting from any ideas, methods, instructions or products referred to in the content.